Limit cycle oscillation prediction for aeroelastic systems with discrete bilinear stiffness

Article · January 2005

CITATIONS
18

READS
233

2 authors:

Gareth Vio
The University of Sydney
121 PUBLICATIONS **774** CITATIONS
SEE PROFILE

Je Cooper
University of Bristol
271 PUBLICATIONS **2,878** CITATIONS
SEE PROFILE

LIMIT CYCLE OSCILLATION PREDICTION FOR AEROELASTIC SYSTEMS WITH DISCRETE BILINEAR STIFFNESS

G. A. Vio[1], and J. E. Cooper[2]

[1]*Manchester School of Engineering, University of Manchester, Oxford Road, Manchester M13 9PL, UK*
Email: gareth.a.vio@manchester.ac.uk
[2]*Manchester School of Engineering, University of Manchester, Oxford Road, Manchester M13 9PL, UK*
Email: jecooper@manchester.ac.uk

Received 5 August 2005; accepted 23 October 2005

ABSTRACT

A methodology is presented that enables the prediction of the limit cycle oscillation behaviour of aeroelastic systems containing discrete bilinear structural nonlinearities using the centre manifold and normal form approaches. The approach extends previous work on aeroelastic systems containing discrete cubic structural nonlinearites. A simple fitting technique is developed to approximate the non-linear stiffness behaviour as a polynomial which enables the normal form method to be used. The approach is demonstrated on several binary and multiple degree of freedom simulated non-linear aeroelastic systems. The predicted LCO amplitudes compare well with the numerical integration results and were far superior in comparison to those predicted using the Harmonic Balance method. Limitations of the new approach are discussed.

Keywords: Normal Form Theory, Harmonic Balance, Aeroelasticity, Bilinear Stiffness.

1 INTRODUCTION

The influence of nonlinearities on modern aircraft and the requirement for more accurate tools for prediction of non-linear effects is becoming increasingly important (Cooper and Noll 1995). These nonlinearities can be due to structural (e.g. freeplay, hysteresis, cubic stiffness), aerodynamic (transonic effects), or control (time delays, control laws) phenomena. It is important to be able to accurately map the dynamics of the system under investigation to distinguish between limit cycle oscillation (LCO), chaotic motion and flutter regions. Although not desirable, LCO phenomena are essentially a fatigue problem whereas flutter is usually catastrophic and must be avoided. Linear structural and aerodynamic models cannot describe or predict LCO phenomena and consequently a large number of (expensive) flight flutter tests may be required to clear a prototype aircraft of these aeroelastic issues.

A further type of structural nonlinearity is the bilinear stiffness which can occur when control systems and spring tab systems are subjected to a preload (Price *et al.* 1995; Lee *et al.* 1999). Other occurrences are when structures become fully tightened once they have been displaced by a certain amount (Breitbach 1978). This latter phenomenon has an effect on the aeroelastic

behaviour of hinged wings (Radcliffe and Cesnik 2001b; Radcliffe and Cesnik 2001a) and will also occur in morphing structures. This paper concentrates on the effect of bilinear type nonlinearities.

There has been much work in recent years (Price *et al.* 1995; Lee *et al.* 1999; Yang and Zhao 1998) devoted towards the characterisation of non-linear aeroelastic behaviour. This work has mainly consisted of simulating the response of aeroelastic systems through numerical simulation, although there are a few known instances of experimental verification (Holden *et al.* 1995; Conner *et al.* 1997). In (Holden *et al.* 1995) the presence of multiple limit cycles was found during the experiment. The full range of periodic and non-periodic motions from a wind tunnel model were compared with numerical integration, giving excellent correlation (Conner *et al.* 1997). In (Virgin *et al.* 1999) the presence of quasi-periodic and chaotic motion was measured in certain speed regions of a wind tunnel model. Some attention has also been directed towards the effect of nonlinearities in aeroservoelastic systems (Dimitriadis and Cooper 1999a; Dimitriadis and Cooper 1999b; Strgnac *et al.* 2000).

Different techniques have been developed to try and reliably map the dynamics of aeroelastic systems. Numerical integration, such as the Runge-Kutta method, is the basis to solve numerically the behaviour of strongly non-linear systems; these methods provide both transient and steady-state responses for prescribed initial conditions but they are time consuming and computationally inefficient. Consequently, much of this work has only considered simplistic aerodynamic models. Extensive efforts are being devoted towards developing coupled solvers that include far more sophisticated aerodynamic modelling, such as full Navier-Stokes solutions (AGARD 1997; Goura *et al.* 2001), particularly in the transonic regime. Such methods, however, incur a significant computational expense

In order to try and reduce the computational load and improve time efficiency of numerical integration, the Cell Mapping technique (Hsu 1980) has been suggested. Greater efficiency was achieved with the introduction of Poincaré planes (Levitas *et al.* 1994) and Cell Mapping has been successfully applied to the solution of aeroelastic systems (Ding *et al.* 2005). The Harmonic Balance method also has been widely used to predict LCOs. This method was introduced by Kryloff & Bogoliuboff (Kryloff and Bogoliuboff 1947) and has been shown (Shen 1959; Luber 2000; Tang *et al.* 1999) to compare reasonably well with results from numerical integration. A version of Harmonic Balance was presented (Lee 1986) in order to study systems with multiple nonlinearities.

It could be argued that such simulations are not predictions; a series of test cases must be considered until the critical conditions are reached, and there is always the possibility that the critical speed may be exceeded or not detected. Developments in the field of applied mathematics have enabled the prediction of stability boundaries for a range of simple non-linear dynamical models (Leung and Qichang 1998), thus eliminating the need for excessive time marching calculations. This approach only recently has been applied to aeroelastic problems where the system model is either known a-priori or is obtained from test. For instance, the use of Normal Form Theory to obtain stability boundaries and LCO characteristics has been successfully applied to a 2DOF system with quasi-steady and unsteady-linear aerodynamics (Sedaghat *et al.* 2000a). The application of the Centre Manifold reduction has been suggested (Grzedzinski 1997; Grzedzinski 1995) to reduce the system equations to as small a dimension as possible. One major assumption of normal form theory is that nonlinearities are continuous and previous work has only considered low order aeroelastic systems with continuous nonlinearities.

Aeroelastic systems often exhibit behaviour that is caused by discrete nonlinearities that can-

not be described with a smooth analytical function e.g. freeplay, bilinear stiffness, hysteresis. Consequently, they have not been considered previously in studies implementing normal form theory. The objective of this paper is to show how Normal Form can be used to predict the stability boundary of non-linear MDOF aeroelastic systems with discrete bilinear stiffness. The key step is to approximate the discrete non-linearity using a simple polynomial. A curve-fitting method is used to determine the coefficients of the polynomial. The method is demonstrated on a number of aeroelastic systems with bilinear stiffness. The results obtained using the normal form approach were compared to numerical simulation and the harmonic balance method. Better comparison was achieved between the Normal Form and numerical simulation results than that achieved using Harmonic Balance. Limitations of the proposed approach are discussed.

2 LCO PREDICTION APPROACH FOR AEROELASTIC SYSTEMS

In this section it is shown how normal form theory can be used to predict the flutter boundary of the aeroelastic systems after the system has been reduced to its critical mode using a centre manifold reduction.

2.1 Centre manifold Reduction

A system of equations can be written in state-space form as

$$\dot{z} = Az + Bg(z) \tag{1}$$

where Az is the linear part and $Bg(z)$ contains the non-linear information of the system. By performing a geometrical transformation the system can be changed to

$$\dot{z} = Jz + Q^{-1}Bg(z) \tag{2}$$

where $J(= Q^{-1}AQ)$ is the Jordan matrix and Q is the modal canonical transformation matrix. The above system can be split into two sets of equations of the form

$$\begin{aligned} \dot{u} &= J_1 u + f_1(u, v) \\ \dot{v} &= J_2 v + f_2(u, v) \end{aligned} \tag{3}$$

where one of the two equations contains the critical mode information. If an appropriate function $v = h(u)$ can be found such that the following relationship is valid

$$\dot{v} = D_u h(u)\dot{u} = D_u h(u)\left[J_1 u + f_1(u, h(u))\right] = J_2 h(u) + f_2(u, h(u)) \tag{4}$$

then only the equation with the critical mode in (3) is required. In the above relation $D_u h(u)$ is the Jacobian of $h(u)$. The function $v = h(u)$ can be approximated in the following form up to third order

$$\begin{aligned} v \;= h(u) = \begin{bmatrix} h_1 \\ h_2 \end{bmatrix} = \; & \begin{bmatrix} a_{10} & a_{01} \\ b_{10} & b_{01} \end{bmatrix} \begin{bmatrix} x_1 \\ x_2 \end{bmatrix} + \begin{bmatrix} a_{20} & a_{11} & a_{02} \\ b_{20} & b_{11} & b_{02} \end{bmatrix} \begin{bmatrix} x_1^3 \\ x_1 x_2 \\ x_2^2 \end{bmatrix} + \\ & \begin{bmatrix} a_{30} & a_{21} & a_{12} & a_{03} \\ b_{30} & b_{21} & b_{12} & b_{03} \end{bmatrix} \begin{bmatrix} x_1^3 \\ x_1^2 x_2 \\ x_1 x_2^2 \\ x_2^3 \end{bmatrix} \end{aligned} \tag{5}$$

where a_{ij} and b_{ij} are unknown coefficients. The Jacobian can be easily determined as follows

$$D_u h(u) = \begin{bmatrix} D_{11} & D_{12} \\ D_{21} & D_{22} \end{bmatrix} = \begin{bmatrix} \frac{\partial h_1}{\partial x_1} & \frac{\partial h_1}{\partial x_2} \\ \frac{\partial h_2}{\partial x_1} & \frac{\partial h_2}{\partial x_2} \end{bmatrix} \tag{6}$$

where

$$\begin{aligned} D_{11} &= a_{10} + 2a_{20}x_2 + 3a_{30}x_1^2 + 2a_{21}x_1x_2 + a_{12}x_2^2 \\ D_{12} &= a_{01} + 2a_{02}x_1 + 3a_{03}x_2^2 + 2a_{12}x_1x_2 + a_{21}x_1^2 \\ D_{21} &= b_{10} + 2b_{20}x_2 + 3b_{30}x_1^2 + 2a_{21}x_1x_2 + b_{12}x_2^2 \\ D_{22} &= b_{01} + 2b_{02}x_1 + 3b_{03}x_2^2 + 2a_{12}x_1x_2 + b_{21}x_1^2 \end{aligned} \tag{7}$$

2.2 Normal Form Theory

Normal form theory (NFT) (Leung and Qichang 1994; Leung and Ge 1995) is used to simplify analytical expressions for non-linear systems. In this case the NFT used is based on the period averaging method. When the averaging method is applied to non-autonomous systems, a coordinate transformation is chosen such that an autonomous system is created through time integration. In this approach the non-linear set of n differential equations

$$\dot{x} = Jx + \epsilon f(x, \epsilon) \quad x \in \Omega \subset R^n, J \in R^{n \times n} \tag{8}$$

is transformed to

$$\dot{y} = \epsilon e^{-Jt} f\left(e^{Jt} y, \epsilon\right) = \epsilon g(y, t, \epsilon) \tag{9}$$

using the transformation

$$x = e^{Jt} y \quad \text{and} \quad \dot{x} = J e^{Jt} y + e^{Jt} \dot{y} \tag{10}$$

where $0 < |x| \ll 1$, $f \in C^{r+1}$ and $f(0, \epsilon) = 0$. Here Ω is the domain that contains the origin and invariant under Γ, and $\Gamma x \in \Omega$ for any $x \in \Omega$, where $\Gamma = \left\{e^{Jt}, t \in R\right\}$.

The period averaged normal form of equation (9) can be constructed using the variable exchange

$$y = \zeta + \sum_{l=1}^{m} \epsilon^l h_l(\zeta, t) \tag{11}$$

that transforms equation (9) to normal form up to order m as

$$\dot{\zeta} = \sum_{k=1}^{m} \epsilon^k f_k^0(\zeta) + O(\epsilon^{m+1}) \tag{12}$$

The geometrical transformation $h_k(\zeta, t)$ in equation (11) is determined from

$$h_k(\zeta, t) = \frac{1}{T} \int_0^{\tau} \tau \left[g_k(\zeta, \tau + t) - f_k^0\right] d\tau \tag{13}$$

and the normal forms $f_k^0(\zeta)$ are given by

$$f_k^0(\zeta) = \frac{1}{T} \int_0^{\tau} g_k(\zeta, \tau) d\tau \tag{14}$$

The function $g_k(\zeta, t)$ is determined by

$$g_k(\zeta,t) = \frac{1}{(k-1)!}\frac{\partial^{k-1}}{\partial \epsilon^{k-1}} g\left(\left(\zeta + \sum_{l=1}^{k-1} \epsilon^l h_l(\zeta,t)\right), t, \epsilon\right)_{\epsilon=0} - \sum_{l=1}^{k-1} h'_{k-1}(\zeta,t) f_l^0(\zeta) \tag{15}$$

in which the prime denotes differentiation with respect to ζ. The time variable disappears from equations (11) and (12) as a result of the averaging process.

2.3 Implementation for discrete non-linearities

One of the major assumptions with Normal Form theory is that the non-linearities are continuous and expressed in the form of a power series

$$F(x) = a_0 + \sum_{i=1}^{n} a_i x^i \tag{16}$$

This assumption means that it is not possible to consider systems containing such non-linearities as freeplay, bilinear stiffnesses, hysteresis, friction, etc. To overcome this difficulty, discrete non-linearities are approximated using a simple polynomial. A simple least squares process was used to fit the characteristic force (F) / displacement (x) behaviour such that

$$\begin{bmatrix} F(x_1) \\ F(x_2) \\ \vdots \\ F(x_i) \end{bmatrix} = \begin{bmatrix} 1 & x_1 & x_1^2 & \cdots & x_1^n \\ \vdots & \vdots & \vdots & \vdots & \vdots \\ \vdots & \vdots & \vdots & \vdots & \vdots \\ 1 & x_i & x_i^2 & \cdots & x_i^n \end{bmatrix} \begin{bmatrix} a_0 \\ a_1 \\ a_2 \\ \vdots \\ a_n \end{bmatrix} \tag{17}$$

Note that all terms of order x^{2n} are negligible if the non-linearity is odd. The fit has to be monotonically increasing otherwise a negative stiffness slope would be present, which is physically impossible.

2.4 Application to aeroelastic systems

Classically, aeroelastic systems can be modelled in terms of a coordinate system q as

$$A\ddot{q} + (\rho V B + D)\,\dot{q} + \left(\rho V^2 C + E\right) q + F(q, \dot{q}) = 0 \tag{18}$$

where A, D, E are the structural inertia, damping and stiffness matrices, B and C represent the aerodynamic damping and stiffness terms. Any non-linearities are modelled through term F. Here we shall assume that the non-linearity is a "soft-centre" bilinear stiffness (Figure 1) of the form

$$F(x) = \begin{cases} K_2 x + (K_1 - K_2)\,\delta & \text{for } x \geq \delta \\ K_1 x & \text{for } -\delta \leq x \leq \delta \\ K_2 x + (K_1 - K_2)\,\delta & \text{for } x \leq -\delta \end{cases} \tag{19}$$

where δ defines displacement governed by the inner stiffness K_1. It is straightforward to rewrite this second order differential equation in the state space formulation of equation (1).

The centre manifold reduction has to be modified when applied to aeroelastic systems. The manifold only exists at the bifurcation point (determined by the existence of two purely imaginary eigenvalues) at speed V_F and here the amplitude of oscillation is zero. We want to determine the LCO amplitude at speeds greater than V_F, but if $V \neq V_F$ the centre manifold does not exist. However, the centre manifold has been proven to exist in the neighbourhood of the equilibrium solution (Hassard *et al.* 1981; Sedaghat *et al.* 2000a). A new parameter has to be introduced to move beyond the bifurcation point in order to find the limit cycle amplitude.

The linear term of equation (1) can be evaluated at $A(V_F)$ where V_F is the flutter speed (the bifurcation point) and at some general speed $V = V_F + \mu$. The solution can then be evaluated near the bifurcation point by using parameter μ as the new speed variable.

3 HARMONIC BALANCE

The harmonic balance method (Dimitriadis 1999; Shen 1959) is used to provide estimates of the stability of the system. The main assumption of this method is that the system admits a limit cycle, which is caused by a non-linear spring. Assuming that the LCO displacement x due to the non-linear spring is sinusoidal with amplitude A, then

$$x = A \sin t \tag{20}$$

Substituting (20) into (19), taking the Fourier expansion and retaining the first order term, we obtain the linearised form of the stiffness, denoted $\hat{K}$, such that

$$\hat{K} = \frac{K_2 - K_1}{\pi} \left(\frac{K_2}{K - 2 - K_1} - 2t_1 - sin(2t_1) \right) \tag{21}$$

where $t_1 = arcsin(\delta/A)$. Equation (21) gives a relationship between the linearised stiffness and limit cycle amplitude $A \geq \delta$. For each stiffness, the flutter equations can be solved to find the critical speeds, and then it is possible to determine the limit cycle amplitude at different speeds (Figure 2).

4 AEROELASTIC MODELS

A number of different simulated aeroelastic systems were used to demonstrate the above approach. The aerodynamics was modelled using a modified strip theory (Hancock *et al.* 1985) which allows for unsteady effects. This approach does not limit the applicability of the work as the objective is to illustrate the methodology on discrete structural nonlinearities. Such nonlinearities can cause LCOs to appear in flight regimes at Mach numbers well below the transonic region (Chen *et al.* 1998). Other work has investigated the use of Normal Form for the prediction of non-linear aeroelastic behaviour in transonic flows (Sedaghat *et al.* 2000b; Sedaghat *et al.* 2000c) subjected to nonlinear aerodynamics forces.

4.1 Binary aeroelastic model

The methodology is demonstrated using the Hancock wing model (Figure 3) (Hancock *et al.* 1985) which consists of a rigid rectangular wing attached at the root by two springs giving rise to bending and torsion motions. The torsional (pitch) spring contained a bilinear stiffness as described in equation (19).

4.2 MDOF aeroelastic model

The second model considered here used a modified Hancock wing model such that bending and torsion modes of the wing were also included. The system considered had two rigid body modes, with a bilinear spring in the rigid torsion mode, and 4 elastic modes (two bending and two torsion).

5 RESULTS AND DISCUSSION

The proposed method was applied to three different aeroelastic systems to test its ability to accurately predict the limit cycle amplitude characteristics. The simple binary system, and two larger systems were considered. In each case, the non-linearity consisted of a strong bilinear stiffness with the following characteristics:

- Binary model with $K_1 = K_\theta$, $K_2 = 2K_\theta$
- MDOF model with $K_1 = K_\theta$, $K_2 = 2K_\theta$
- MDOF model with $K_1 = K_\theta$, $K_2 = 4K_\theta$

where $K_\theta = 6.5 * 10^5$ Nm/rad for the binary model and $K_\theta = 1.2 * 10^3$ Nm/rad for the MDOF models, K_1 is the inner torsional stiffness and K_2 is the outer torsional stiffness.

The bifurcation plots, obtained by applying an initial displacement to the systems at a range of wind speeds (Figs. 4, 5 and 6), show the presence of limit cycles of period-1 for all of the systems considered. The characteristic jump phenomena caused by the presence of discrete nonlinearities is clearly present at the bifurcation point. The amplitudes grow steadily until flutter is encountered in all cases at a speed defined by the linear flutter speed related to the outer stiffness value (K_2) of the non-linearity.

The non-linear force/displacement behaviour was fitted using varying orders of polynomial to find the best fit (Figs. 7 and 8). The fitted region was chosen to cover displacements relating to all the inner stiffness and a small part of the outer stiffness. This restriction is due to the NFT being only valid in the proximity of the bifurcation point. The fit also captures the turning points better than if a wider range were considered, which is critical in obtaining an accurate solution.

The flutter speed using the linear fitted stiffness term (coefficient a_1 in equation (17)) was calculated (Sedaghat *et al.* 2001). This gives the speed at which the bifurcation occurs and is also used during the reduction process. A second order approximation was employed to find the normal forms in equation (15). Solutions using the Harmonic Balance method were also obtained. Both LCO amplitude predictions were compared with numerical integration results using the ODE45 routine in Matlab and Simulink which is based on the explicit Dormand-Prince pair Runge-Kutta (4,5) formula (Dormand and Prince 1980).

There are some interesting effects that arise as a consequence of the fitting process. If we look at the curve-fitting solution in Figures 9 and 10 beyond the specified displacement range, it can be seen that the fit turns back on itself. In these regions, the non-linearity becomes destabilizing, and this has a major effect on the solutions obtained.

Figures 11, 12 and 13 show the LCO predictions using the NFT. The curve shows good agreement with the integration results (Figs. 11, 12) with differences of less than a degree. Excellent

agreement is achieved for the results in Figure 13. Although one part of the solution gives a good agreement with the integration results, a further LCO branch is created corresponding to the destabilizing part of the curve-fit. Consequently, we can only regard what happens within the fitted region as being a true solution. The lowest branch should always be taken as this is the stable set of results.

Figures 14, 15 and 16 compare the numerical integration results with the harmonic balance prediction. The harmonic balance fails to capture correctly the LCO amplitudes for the binary system. Better agreement is obtained for the 6dof system (Figure 15). In the first case the harmonic balance capture the correct trend of the bifurcation, but underpredicts the amplitude throughout most of the bifurcation range, giving only accurate results at the beginning and end point, as expected. The same behaviour can be seen in Figure 14. In Figure 16 good agreement is achieved between the numerical integration and Harmonic Balance solution for the third case considered, where there is only a slight under-prediction of the true LCO amplitude. These results show that although Harmonic Balance can give good predictions, this is not true for all cases. In the cases shown in this paper, the Normal Form solution consistently gives more accurate solutions, and this has been found in other cases not shown here.

In Figure 17, the Harmonic Balance, Normal Form and numerical integration solutions are compared for the simple binary system. It is evident that the normal form solution gives a much more accurate solution than Harmonic Balance in the near vicinity of the bifurcation. Although the normal form predicts the start of the bifurcation 1 m/s later than the actual bifurcation speed, this difference is due to the fitting method. Improvements in the curvefitting method could see this difference reduced. The amplitude predicted is a perfect match to the numerical integration up to the point where we exit the range of the curvefitted region. The difference between the Harmonic Balance and Normal Form methods can be due to the fact that the Harmonic Balance method only takes into account a single frequency to describe the solution. Nonlinearities contain different frequencies in their spectrum, and in systems that contains discrete nonlinearities such as bilinear stiffness, an increased number of frequencies will be present (Thomsen 1997). The Normal Form eliminates all the redundant frequencies, but retains the ones that characterise the system, i.e. the resonant terms.

All the results presented here have been obtained by using a simplified version of the reduction process. Only the critical terms were retained to obtain the critical mode with a third order approximation. Results should improve when using the full reduction method and higher order approximation during the normal form procedure, and this is currently being considered.

6 APPLICATION TO FREEPLAY AND HYSTERETIC NONLINEARITIES

Having demonstrated the applicability of the approach to bilinear non-linearites, the next step is to consider freeplay and hysteretic nonlinearities. A problem that occurs with the curvefitting process described above to freeplay nonlinearities is that a negative linear coefficient tends to be found when applied stiffness/displacement such as in Figure 1 are fitted with the inner stiffness $K_1 = 0$. For low order aeroelastic systems the instability mechanism is non-oscillatory and consequently the system goes statically unstable before any LCO occur. Figure 18 shows the relationship between the inner stiffness and the flutter speed for the binary system considered in this paper, and it can be seen that a minimum value of inner stiffness is required for flutter to occur.

Hysteretic non-linearities lead to stiffness / displacement behaviours that are made up of two

distinct bilinear stiffness paths. The procedure described above cannot deal directly with this type of non-linearity.

Work is progressing to extend of the Centre Manifold / Normal Form approach to address both types of non-linearities.

7 CONCLUSIONS

This paper has assessed the ability of using the Centre Manifold and Normal Form techniques for the prediction of limit cycle amplitudes when discrete structural nonlinearities are present in an aeroelastic system. A fitting technique was used to approximate the non-linear stiffness behaviour as a polynomial, thus enabling the use of the normal form technique. The methodology was demonstrated on a binary simulated non-linear aeroelastic system with bilinear stiffness to assess the ability of the centre manifold and normal form to predict LCO amplitudes. The predictive capabilities were also tested on multiple-degree-of-freedom systems with different levels of bilinear stiffness. All the LCO predictions using the proposed method compared well with the numerical integration results and were superior and more consistent in their result than the Harmonic Balance method.

8 ACKNOWLEDGMENTS

The authors would like to acknowledge the support received by the Engineering and Physical Sciences Research Council and BAE Systems.

REFERENCES

AGARD (1997). Numerical unsteady aerodynamic and aeroelastic simulation. Technical report, AGARD-NATO, RTO, Aalborg, Denmark.

Breitbach E (1978). Effects of structural nonlinearities on aircraft vibration and testing. Report R-665, AGARD.

Chen PC, Sarbaddi D, and Liu DD (1998). Limit cycle-oscillation studies of a fighter with external stores. *Proceedings of the* 39^{th} *AIAA/ASME/AHS Structures, Structural Dynamics & Materials Conference*, Long Beach, California.

Conner MD, Tang DM, Dowell EH, and Virgin LN (1997). Nonlinear behaviour of a typical airfoil section with control surface freeplay: a numerical and experimental study. *Journal of Fluids and Structures 11*, pp. 89–109.

Cooper JE and Noll TT (1995). Technical evaluation report on the 1995 specialists' meeting on advanced aeroservoelastic testing and data analysis. Conference Proceedings CP-566, AGARD.

Dimitriadis G (1999). *Investigation of nonlinear aeroelastic systems*. Ph. D. thesis, University of Manchester.

Dimitriadis G and Cooper JE (1999a). Characterisation of nonlinear aeroservoelastic behaviour. *RTO Meeting Proceedings 36, Structural aspects of flexible aircraft control*, Ottawa, Canada.

Dimitriadis G and Cooper JE (1999b). Limit cycle oscillation control and suppression. *Aeronautical Journal 103*, pp. 257–263.

Ding Q, Cooper JE, and Leung AYT (2005). Application of an improved cell mapping method to bilinear stiffness aeroelastic systems. *Journal of Fluids and Structures 20*(1), pp. 35–49.

Dormand JR and Prince PJ (1980). A family of embedded runge-kutta formulae. *Journal of Computational and Applied Mathematics 6*, pp. 19–26.

Goura GSL, Badcock KJ, Woodgate MA, and Richards BE (2001). Evaluation of methods for the time marching analysis of transonic aeroelasticity. 39^{th} *AIAA Applied Aerodynamics Conference*.

Grzedzinski J (1995). Flutter calculation of an aircraft with non-linear structure based on center-manifold reduction. *Proceedings of the CEAS International Forum on Aeroelasticity and Structural Dynamics*, Manchester, UK.

Grzedzinski J (1997). Subsonic flutter calculation of an aircraft with non-linear control system based on center-manifold reduction. *Archive of Mechanics 49*(1), pp. 3–26.

Hancock GJ, Wright JR, and Simpson A (1985). On the teaching of the principle of wing flexure-torsion flutter. *Aeronautical Journal*, pp. 285–305.

Hassard BD, Kazarinoff ND, and Wan Y-H (1981). *Theory of Hopf bifurcation*. Cambridge University Press Books.

Holden M, Brazier R, and Cal A (1995). Effect of structural non-linearities on a tailplane flutter model. *Proceedings of the CEAS International Forum on Aeroelasticity and structural dynamics*, Manchester, UK.

Hsu CS (1980). A theory of cell-to-cell mapping for dynamical systems. *Journal of Applied Mechanics 47*, pp. 931–939.

Kryloff N and Bogoliuboff N (1947). *Introduction to nonlinear mechanics (a free translation by S Lefschets)*. Princeton University Press Books.

Lee BHK, Price SJ, and Wong YS (1999). Nonlinear aeroelastic analysis of airfoils: bifurcation and chaos. *Progress in Aerospace Sciences 35*, pp. 205–334.

Lee CL (1986). An iterative procedure for nonlinear flutter analysis. *AIAA Journal 24*(3), pp. 833–840.

Leung AYT and Ge T (1995). An algorithm for higher order hopf normal form. *Journal of Shock and Vibration 2*(4), pp. 307–319.

Leung AYT and Qichang Z (1994). Normal form analysis of hopf bifurcation exemplified by duffing's equation. *Journal of Shock and Vibration 1*(3), pp. 233–240.

Leung AYT and Qichang Z (1998). Higher order normal form and period averaging. *Journal of Sound and Vibration 217*(5), pp. 795–806.

Levitas J, Weller T, and Singer J (1994). Poincaré-like cell mapping for non-linear dynamical systems. *Journal of Sound and Vibration 176*(5), pp. 641–662.

Luber WG (2000). Flutter prediction on a combat aircraft involving freeplay on control surfaces. *International Conference on Noise and Vibration Engineering, ISMA 2000*, Leuven, Belgium.

Price SJ, Alighanbari H, and Lee BHK (1995). The aeroelastic response of a 2 dimensional aerofoil with bilinear and cubic structural non-linearities. *Journal of Fluids and Structures 9*, pp. 175–193.

Radcliffe TO and Cesnik CES (2001a). Aeroelastic behaviour of multi-hinged wings. *Proceedings of the CEAS International Forum on Aeroelasticity and structural dynamics*, Madrid, Spain.

Radcliffe TO and Cesnik CES (2001b). Aeroelastic response of multi-segmented hinged wings. *Proceedings of the* 42^{nd} *AIAA/ASME/ASCE/AHS/ASC Structures, Structural Dynamics & Materials Conference*, Seattle, Washington.

Sedaghat A, Cooper JE, Leung AYT, and Wright JR (2000a). Limit cycle oscillation prediction for aeroelastic systems with continuous non-linearities. *Proceedings of the* 41^{st} *AIAA/ASME/ASCE/AHS/ASC Structures, Structural Dynamics & Materials Conference*, Atlanta, Georgia.

Sedaghat A, Cooper JE, Leung AYT, and Wright JR (2000b). Modelling of non-linear aerodynamics during limit cycle oscillations. *International Conference on Noise and Vibration Engineering, ISMA 2000*, Leuven, Belgium.

Sedaghat A, Cooper JE, Leung AYT, and Wright JR (2000c). Prediction of non-linear aeroelastic instabilities. *ICAS Congress*, Harrogate, UK.

Sedaghat A, Cooper JE, Leung AYT, and Wright JR (2001). Estimation of the hopf bifurcation point for aeroelastic systems. *Journal of Sound and Vibration 248*(1), pp. 31–42.

Shen SF (1959). An approximate analysis of nonlinear flutter problem. *Journal of the Aerospace Sciences*, pp. 25–32.

Strgnac TW, Thompson DE, and Kurdila AJ (2000). Identification and control of limit cycle oscillations in aeroelastic systems. *Journal of Guidance, Control and Dynamics 23*(6), pp. 1127–1133.

Tang DM, Dowell EH, and Virgin LN (1999). Limit cycle behavior of an airfoil with a control surface. *Journal of Fluids and Structures 12*, pp. 839–858.

Thomsen JJ (1997). *Vibration and stability order and chaos*. McGraw-Hill.

Virgin LN, Dowell EH, and Conner MD (1999). On the evolution of deterministic non-periodic behavior of an airfoil. *International Journal of Non-Linear Mechanics 34*, pp. 499–514.

Yang ZC and Zhao LC (1998). Analysis of limit cycle flutter of an airfoil in incompressible flow. *Journal of Sound and Vibration 123*(1), pp. 1–13.

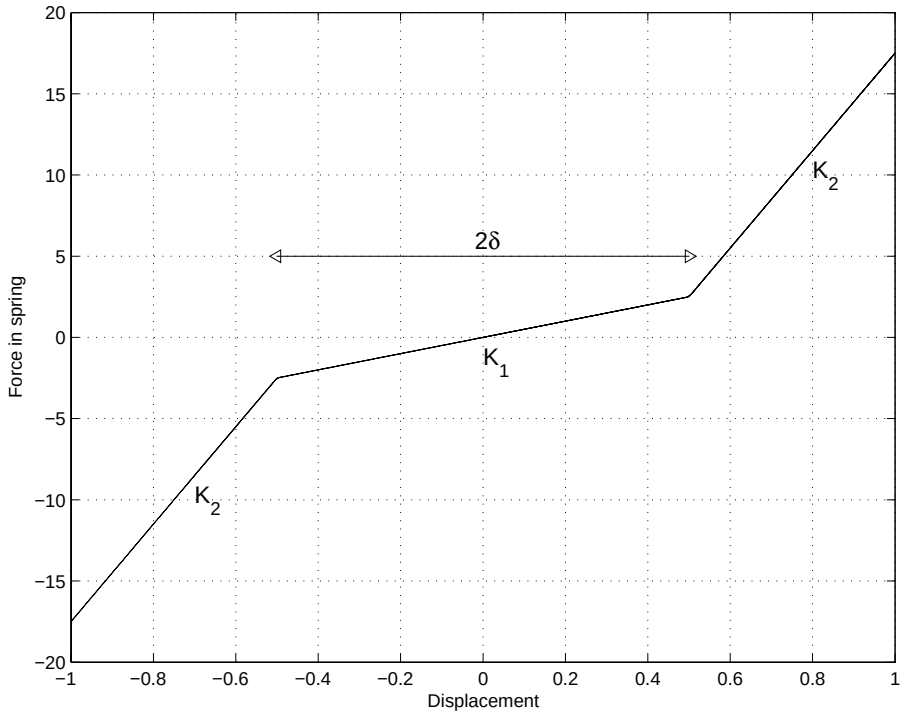

Figure 1: Bilinear stiffness versus displacement

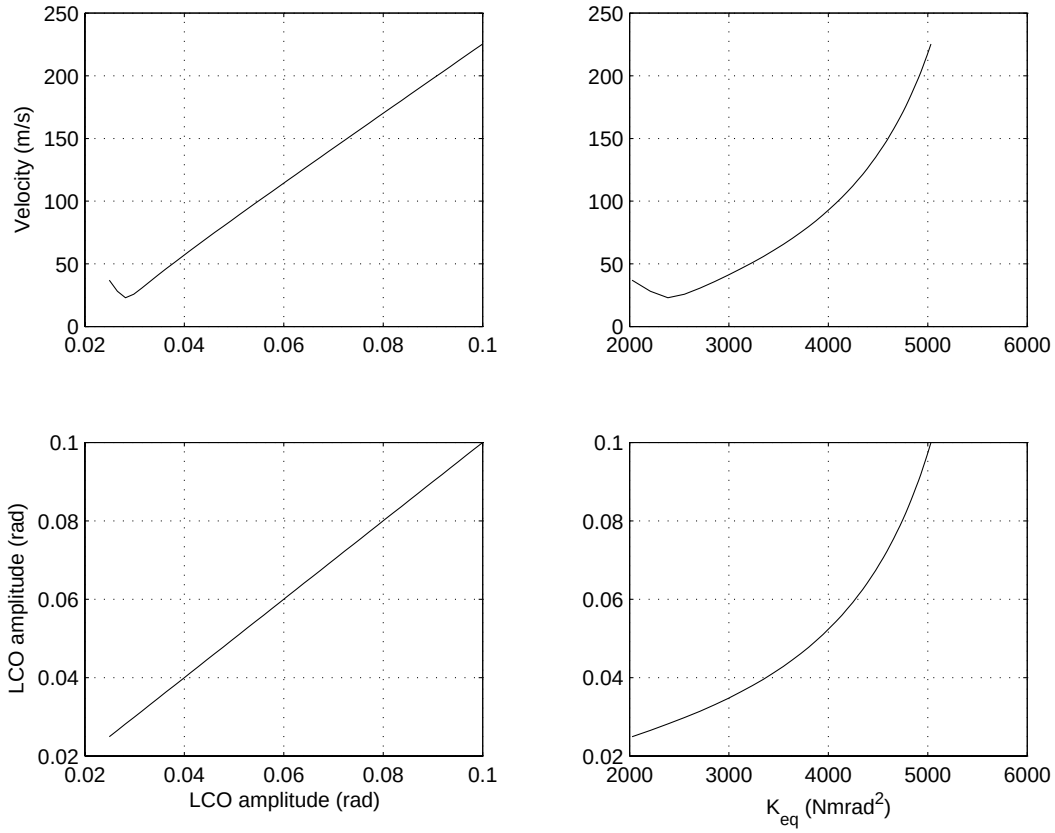

Figure 2: Harmonic Balance result. Binary model

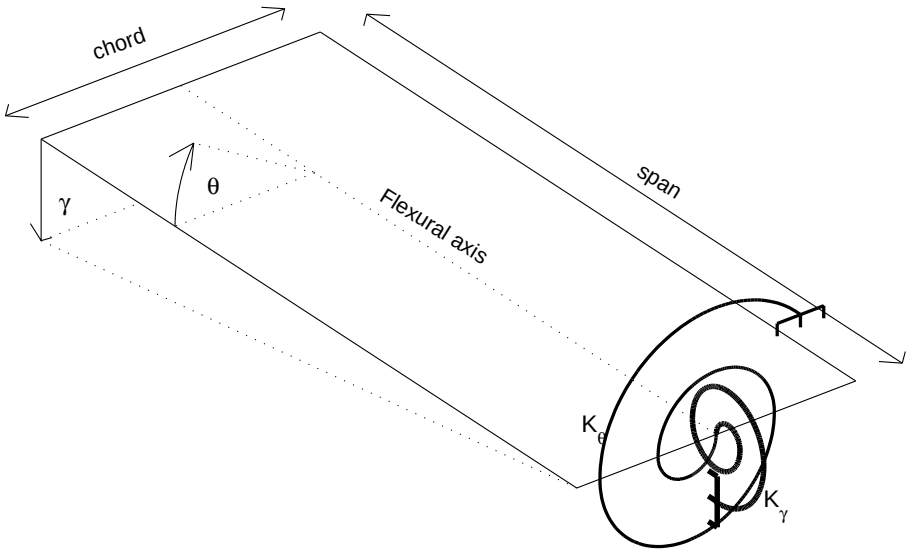

Figure 3: Hancock wing model

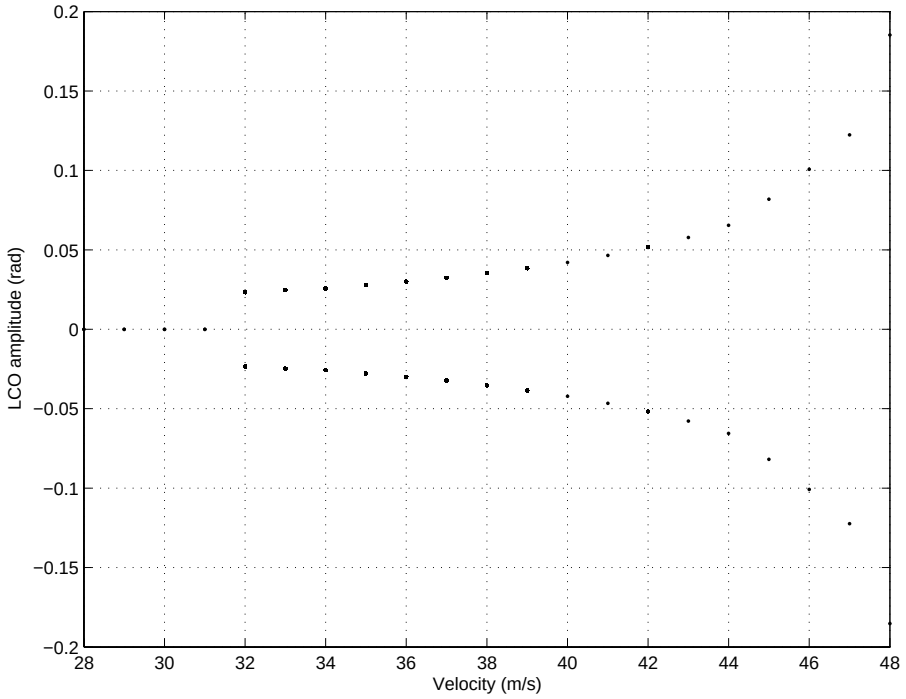

Figure 4: Bifurcation plot for 2DOF system with bilinear stiffness $(K_2 = 2K_1)$

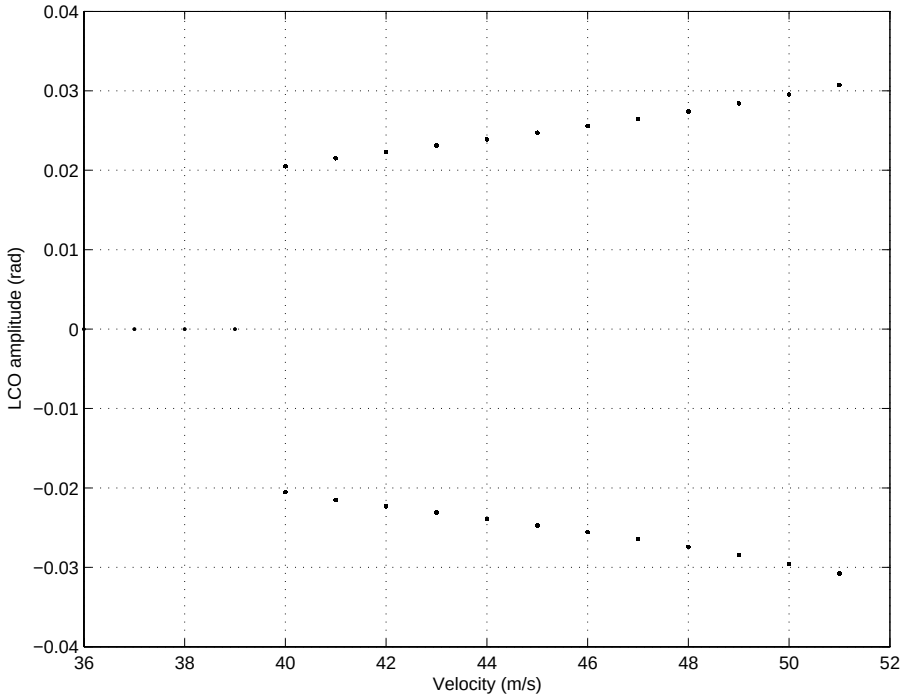

Figure 5: Bifurcation plot of 6DOF system with bilinear stiffness $(K_2 = 4K_1)$

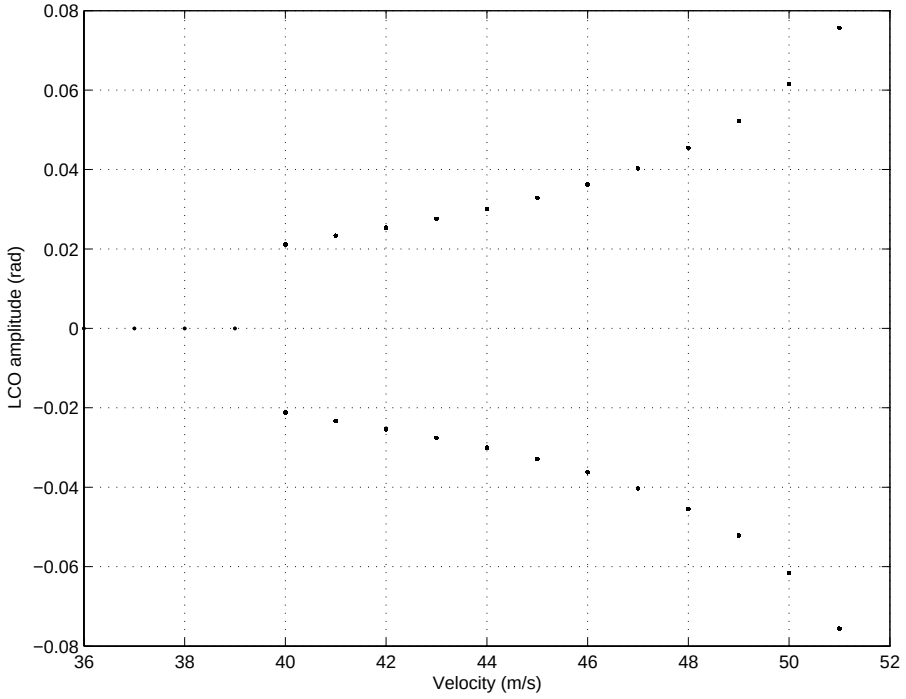

Figure 6: Bifurcation plot of 6DOF system with bilinear stiffness $(K_2 = 2K_1)$

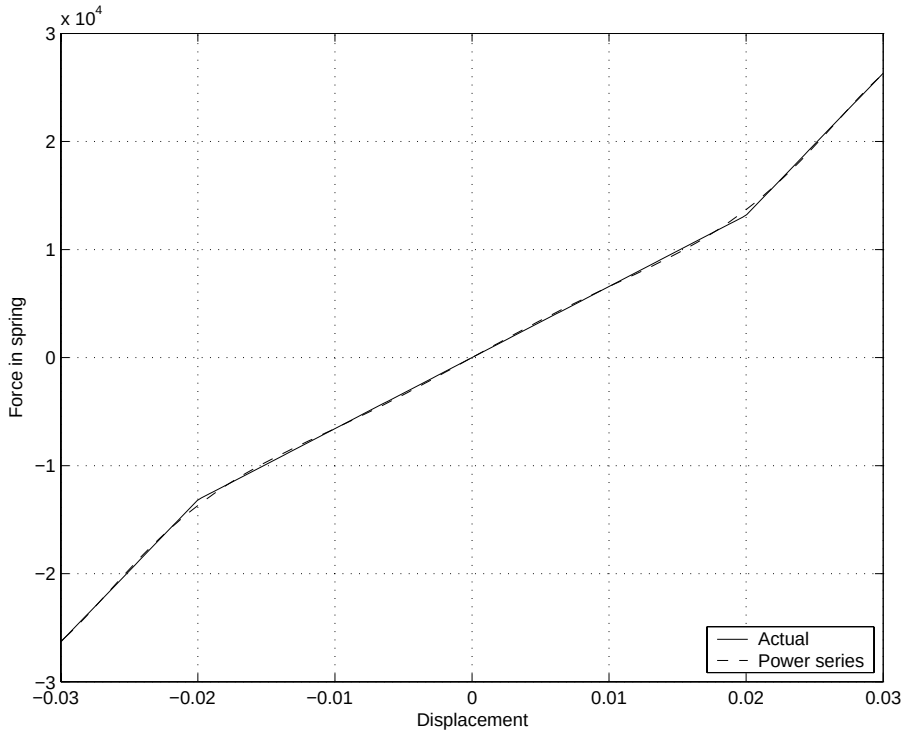

Figure 7: Bilinear stiffness approximation using a power series for 2DOF system. Polynomial of order n=7

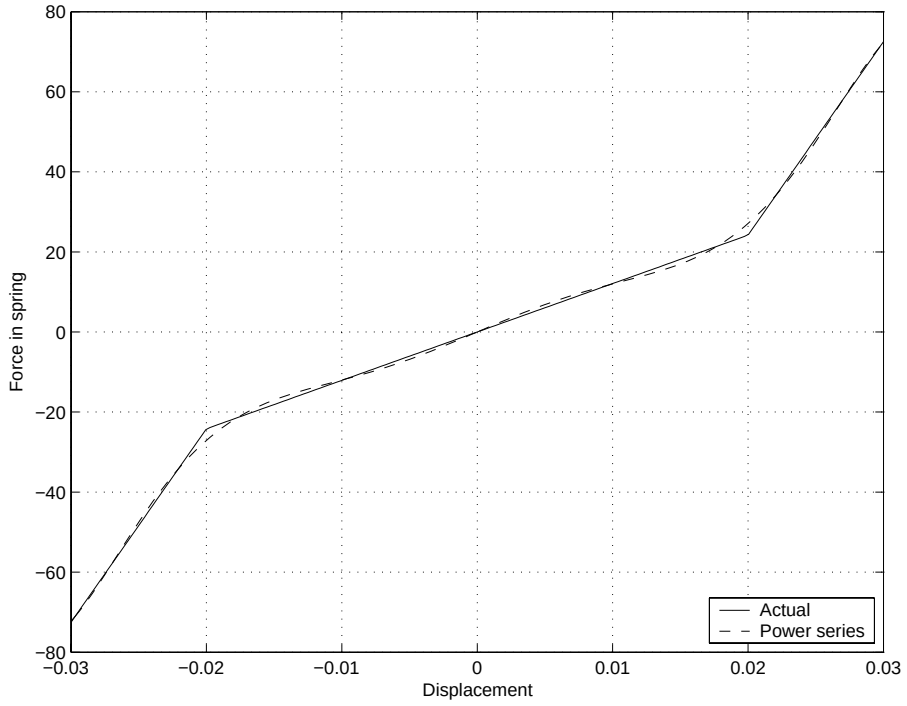

Figure 8: Bilinear stiffness approximation using a power series for 6DOF system. Polynomial of order n=7

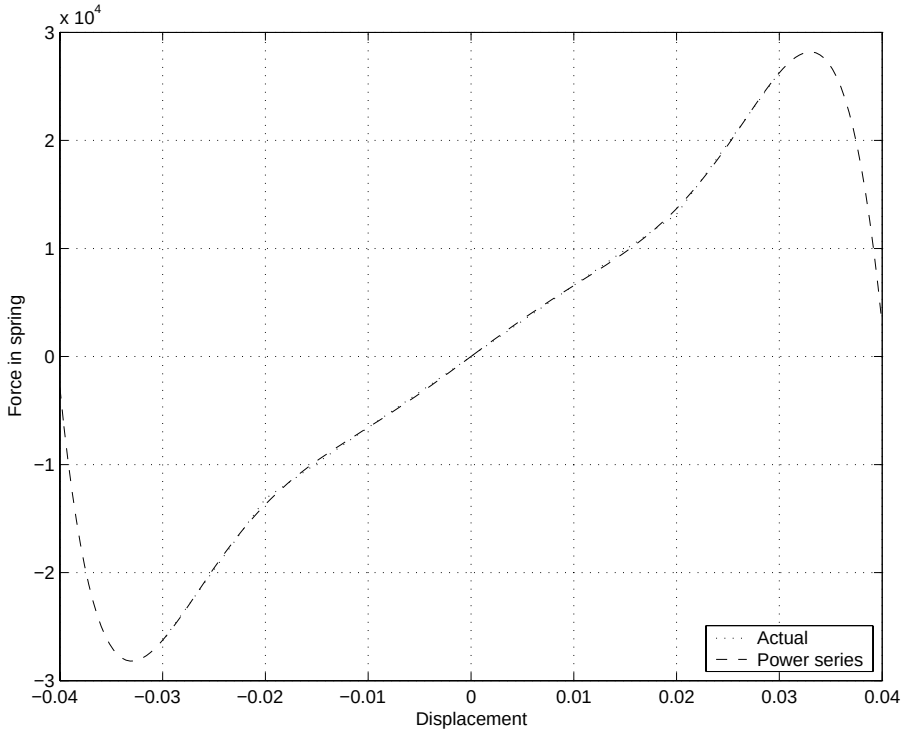

Figure 9: Extrapolation of curve beyond maximum fitted point for 2DOF system

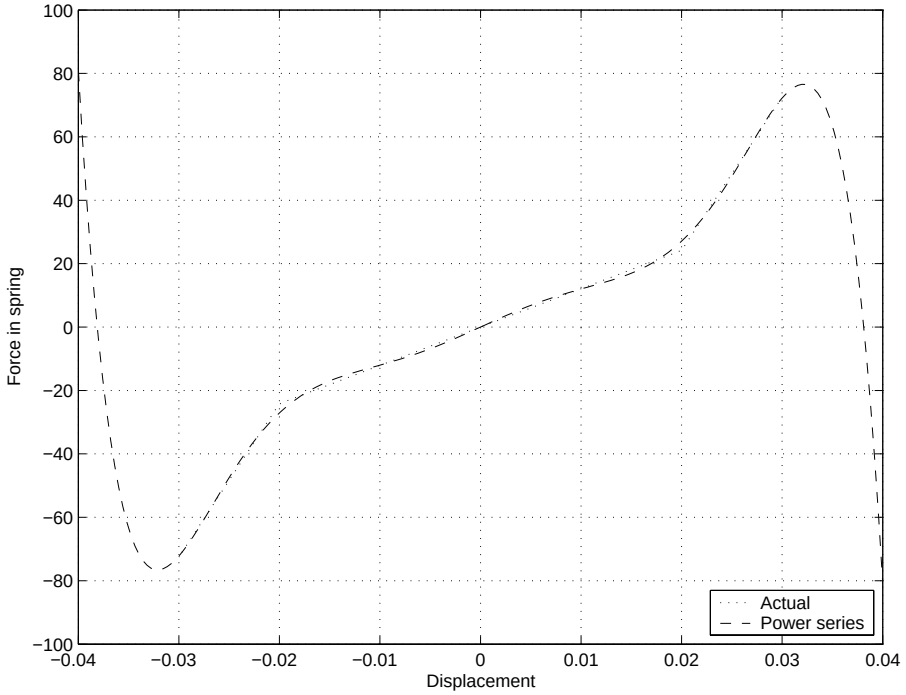

Figure 10: Extrapolation of curve beyond maximum fitted point for 6DOF system

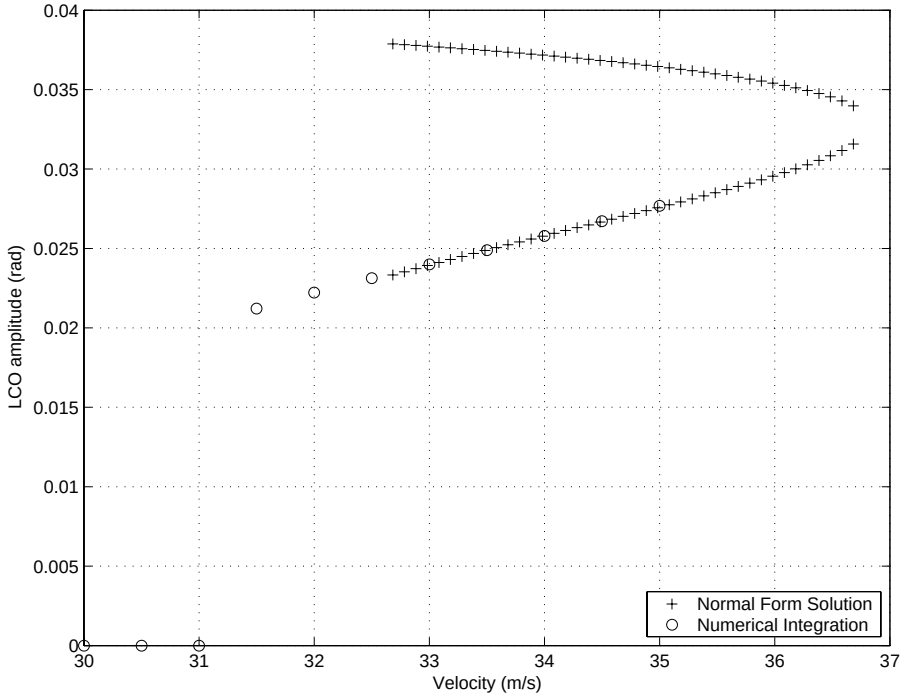

Figure 11: Comparison between NFT and numerical integration for 2DOF system with bilinear stiffness $(K_2 = 2K_1)$

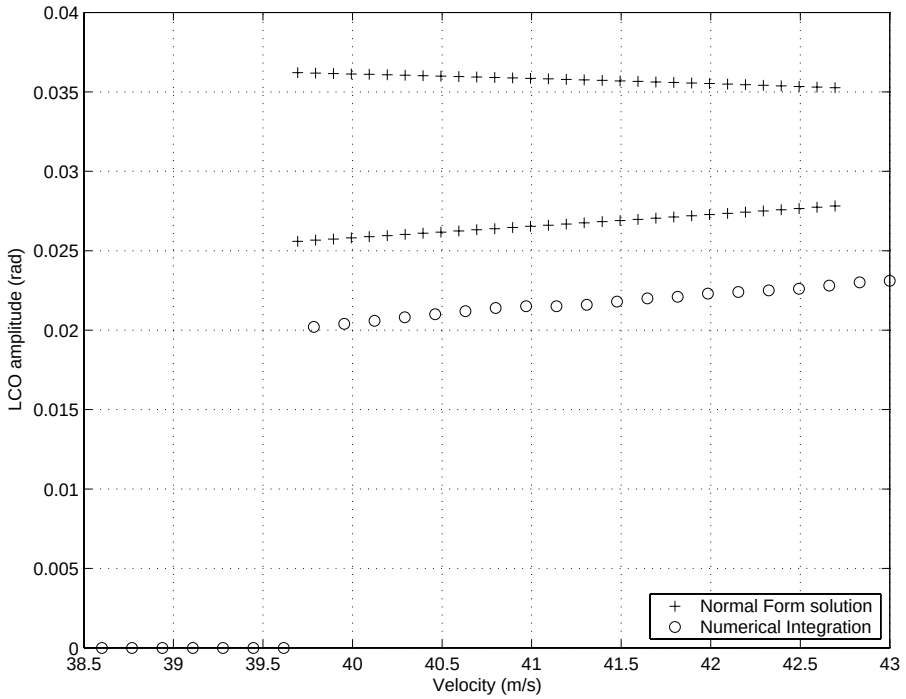

Figure 12: Comparison between NFT and numerical integration for 6DOF system with bilinear stiffness $(K_2 = 4K_1)$

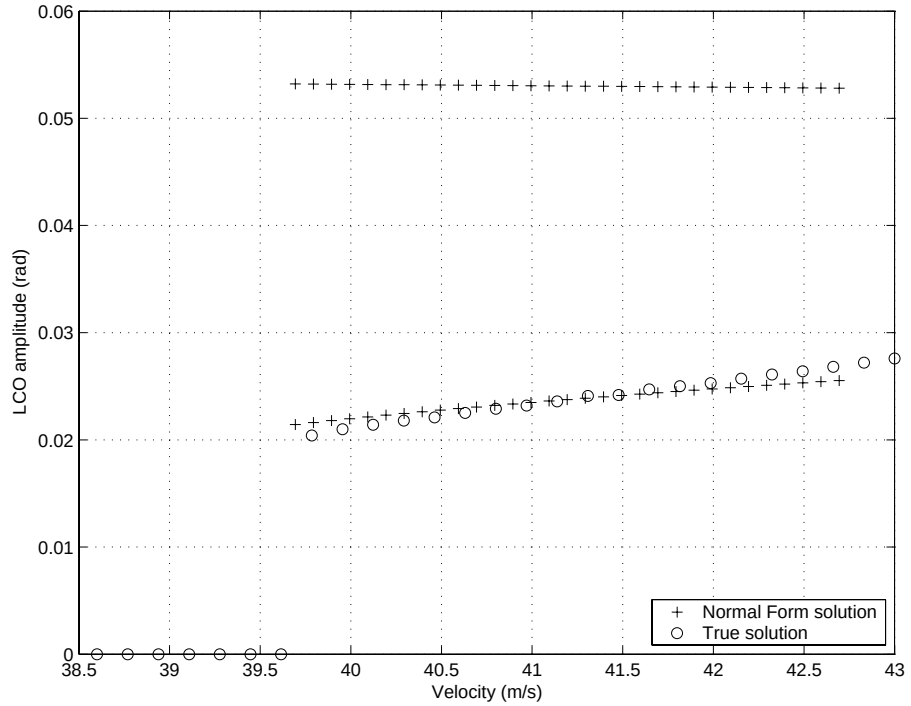

Figure 13: Comparison between NFT and numerical integration for 6DOF system with bilinear stiffness $(K_2 = 2K_1)$

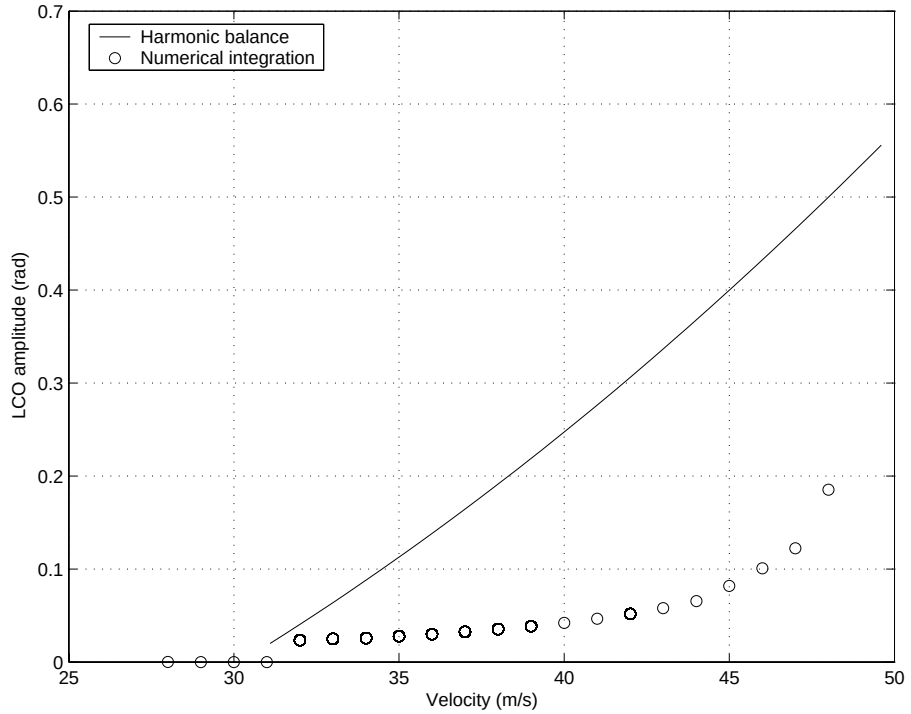

Figure 14: Comparison between HB and numerical integration for 2DOF system with bilinear stiffness $(K_1 = 2K_2)$

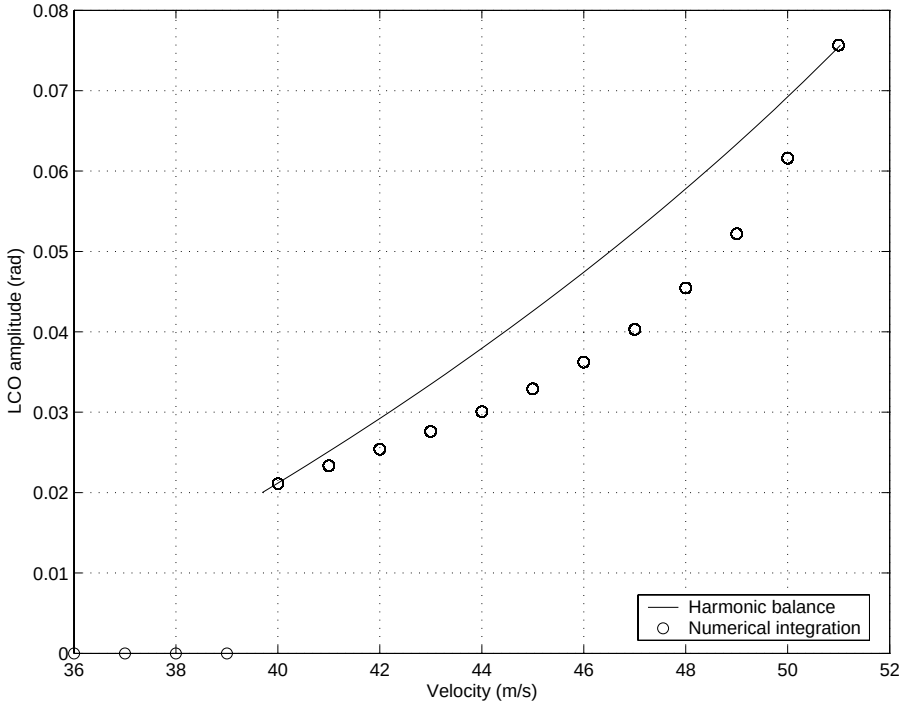

Figure 15: Comparison between harmonic balance and numerical integration for 6DOF system with bilinear stiffness $(K_1 = 2K_2)$

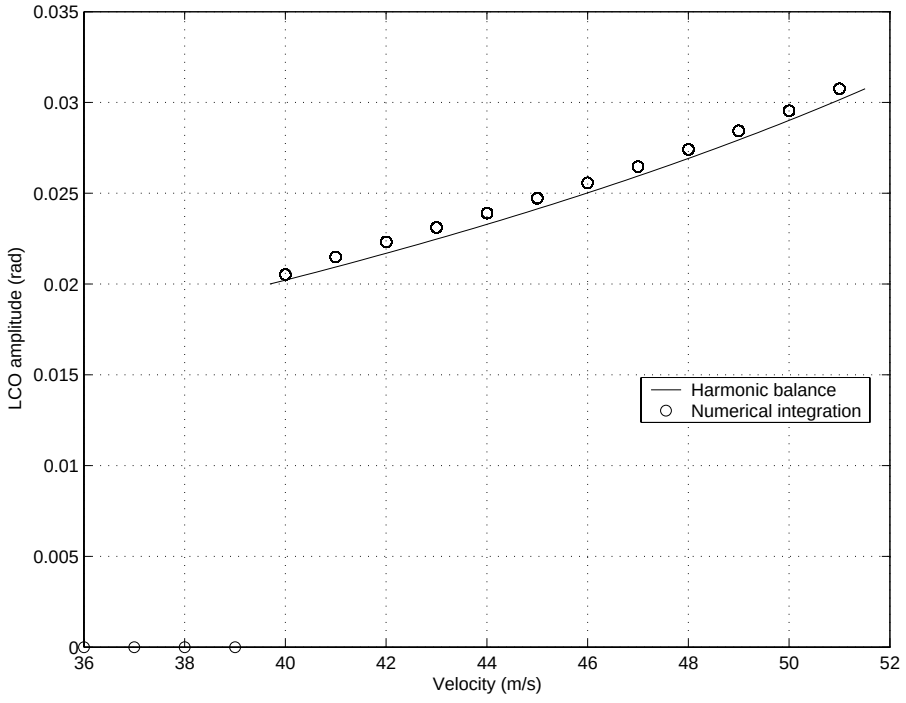

Figure 16: Comparison between HB and numerical integration for 6DOF system with bilinear stiffness $(K_1 = 4K_2)$

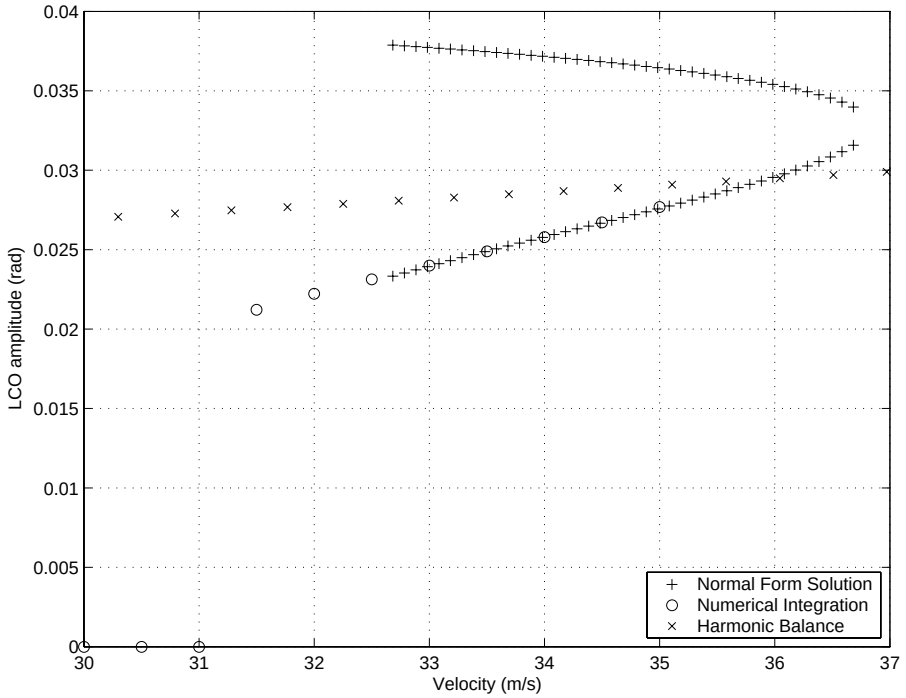

Figure 17: Comparison between normal form, harmonic balance and numerical integration for 2DOF system with bilinear stiffness $(K_1 = 2K_2)$

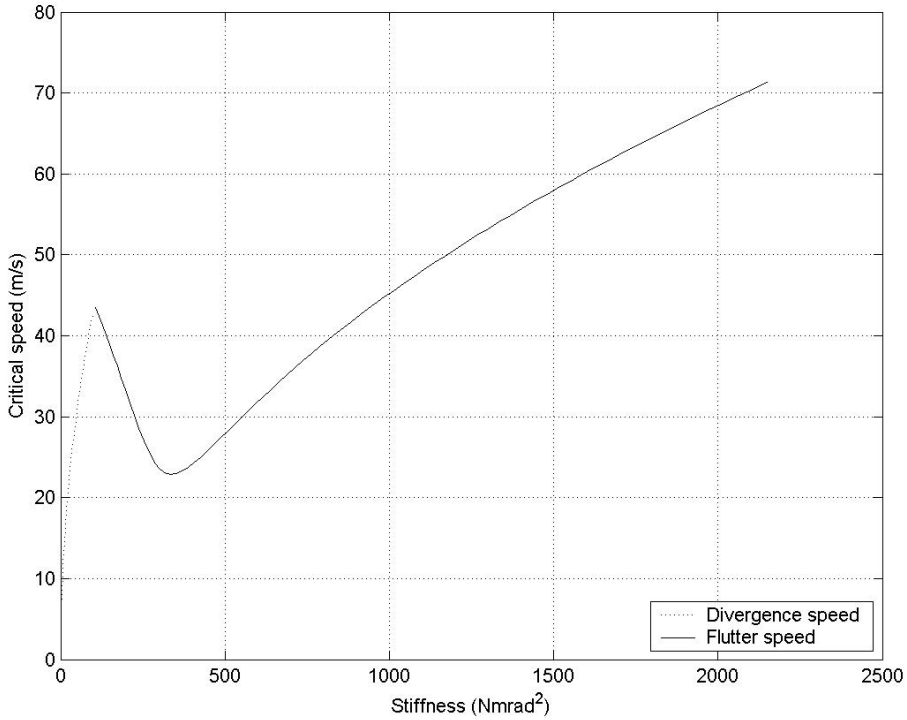

Figure 18: Effect of changing the torsional stiffness on flutter speed for 2DOF system